

# Protective effect of 18 $\beta$ -glycyrrhetic acid against H<sub>2</sub>O<sub>2</sub>-induced injury in Schwann cells based on network pharmacology and experimental validation

DI ZHANG<sup>1\*</sup>, JIANXIN SUN<sup>1\*</sup>, SHIQUAN CHANG<sup>1</sup>, XING LI<sup>1</sup>, HUIMEI SHI<sup>1</sup>, BEI JING<sup>1</sup>,  
YACHUN ZHENG<sup>1</sup>, YI LIN<sup>1</sup>, GUOQIANG QIAN<sup>2</sup>, YUWEI PAN<sup>3</sup> and GUOPING ZHAO<sup>1</sup>

<sup>1</sup>College of Traditional Chinese Medicine, Jinan University, Guangzhou, Guangdong 510632;

<sup>2</sup>College of Traditional Chinese Medicine, Guangdong Pharmaceutical University, Guangzhou, Guangdong 510006;

<sup>3</sup>Preventive Treatment of Disease, Tianhe Traditional Chinese Medicine Hospital, Guangzhou, Guangdong 510665, P.R. China

Received May 28, 2021; Accepted August 3, 2021

DOI: 10.3892/etm.2021.10676

**Abstract.** The aim of the present study was to assess the protective effects of 18 $\beta$ -GA against hydrogen peroxide (H<sub>2</sub>O<sub>2</sub>)-induced injury. First, the SMILES annotation for 18 $\beta$ -GA was used to search PubChem and for reverse molecular docking in Swiss Target Prediction, the Similarity Ensemble Approach Search Server and the TargetNet database to obtain potential targets. Injury-related molecules were obtained from the GeneCards database and the predicted targets of 18 $\beta$ -GA for injury treatment were selected by Wayne diagram analysis. Subsequently, Kyoto Encyclopedia of Genes and Genomes analysis was performed by WebGestalt. The experimental cells were assorted into control, model, 10  $\mu$ M SB203580-treated, 5  $\mu$ M 18 $\beta$ -GA-treated and 10  $\mu$ M 18 $\beta$ -GA-treated groups. Hoechst 33258 staining was performed and intracellular reactive oxygen species (ROS) levels, cell apoptosis, Bcl-x1, Bcl-2, Bad, Bax, cleaved-caspase 3, cleaved-caspase 7, transient receptor potential ankyrin 1 (TRPA1) and transient receptor potential vanilloid 1 (TRPV1) levels, as well as p38 MAPK phosphorylation were measured. The ‘Inflammatory mediator

regulation of TRP channels’ pathway was selected for experimental verification. The results indicated that 10  $\mu$ M 18 $\beta$ -GA significantly increased cell viability as compared with the H<sub>2</sub>O<sub>2</sub>-treated model group. As suggested by the difference in intracellular ROS fluorescence intensity, 18 $\beta$ -GA inhibited H<sub>2</sub>O<sub>2</sub>-induced ROS production in Schwann cells. Hoechst 33258 staining indicated that 18 $\beta$ -GA reversed chromatin condensation and the increase in apoptotic nuclei following H<sub>2</sub>O<sub>2</sub> treatment. Furthermore, flow cytometry suggested that 18 $\beta$ -GA substantially inhibited H<sub>2</sub>O<sub>2</sub>-induced apoptosis. Pre-treatment with 18 $\beta$ -GA obviously reduced Bad, Bax, cleaved-caspase3, cleaved-caspase 7, TRPA1 and TRPV1 levels and p38 MAPK phosphorylation after H<sub>2</sub>O<sub>2</sub> treatment and increased Bcl-2 and Bcl-x1 levels. In conclusion, 18 $\beta$ -GA inhibited Schwann cell injury and apoptosis induced by H<sub>2</sub>O<sub>2</sub> and may be a potential drug to prevent peripheral nerve injury.

## Introduction

18 $\beta$ -Glycyrrhetic acid (18 $\beta$ -GA) and 18 $\alpha$ -GA are the active components of *Glycyrrhiza glabra* (1). As the natural availability of the 18 $\alpha$ -GA isomer is low and that of 18 $\beta$ -GA is higher, there is a greater research focus on 18 $\beta$ -GA (2). Previous studies have demonstrated the diverse favourable effects of 18 $\beta$ -GA, including its hepatoprotective, renoprotective, antioxidant and inflammation relief effects (3-5). Zhou *et al* (6) indicated that 18 $\beta$ -GA suppressed autoimmune encephalomyelitis by inhibiting the activation of microglia and facilitating remyelination via inhibition of the MAPK signalling pathway. Oztanir *et al* (7) suggested that treatment with 18 $\beta$ -GA for 10 days after cerebral ischaemia/reperfusion (I/R) altered the neurodegenerative effect of I/R on brain tissue due to its powerful antioxidant effect and capability to scavenge radicals. Kao *et al* (8) indicated that 18 $\beta$ -GA protected PC12 cells from 6-hydroxydopamine-induced harm through PI3K/Akt signalling and the Bcl-2 family. However, the protective mechanism of 18 $\beta$ -GA in Schwann cells has remained elusive. As Schwann cells have a vital impact on nerve repair (9), the present study explored the protective capacity of 18 $\beta$ -GA against H<sub>2</sub>O<sub>2</sub>-induced injury in Schwann cells.

**Correspondence to:** Professor Guoping Zhao, College of Traditional Chinese Medicine, Jinan University, 601 Huangpu Avenue West, Guangzhou, Guangdong 510632, P.R. China  
E-mail: tguo428@jnu.edu.cn

Dr Yuwei Pan, Preventive Treatment of Disease, Tianhe Traditional Chinese Medicine Hospital, 9 Tangshi Road, Guangzhou, Guangdong 510665, P.R. China  
E-mail: pywyv@foxmail.com

\*Contributed equally

**Abbreviations:** H<sub>2</sub>O<sub>2</sub>, hydrogen peroxide; ROS, reactive oxygen species; 18 $\beta$ -GA, 18 $\beta$ -glycyrrhetic acid; TRPA1, transient receptor potential ankyrin 1; TRPV1, transient receptor potential vanilloid 1

**Key words:** 18 $\beta$ -glycyrrhetic acid, hydrogen peroxide, H<sub>2</sub>O<sub>2</sub>, p38 MAPK, Schwann cells, network pharmacology

Peripheral nerve injury is a common problem and may result in severe disability and an economic burden (10). Despite the fact that peripheral nerve cells have a specific regenerative ability, functional prognosis is not optimal (11). Schwann cells are proliferative glial cells in the peripheral nervous system and they are essential for nerve repair after injuries to maintain normal nerve function (12). Increasing evidence indicates that Schwann cell death is the major cellular event in the pathogenesis of peripheral nerve injuries, which tend to manifest in the form of apoptosis (13). In addition, oxidative stress after injury has a considerable role in neuronal death. The most important genes associated with apoptosis are proteins of the Bcl family and caspases (14,15). Su *et al* (3) indicated that 18 $\beta$ -GA lessened the severity of radiation-induced skin injury and decreased inflammatory infiltration and the levels of TNF- $\alpha$ , IL-1 $\beta$  and IL-6 in dermal tissues by decreasing NADPH oxidase activity and reactive oxygen species (ROS) production and suppressing the activation of p38 MAPK and NF- $\kappa$ B signalling. 18 $\beta$ -GA demonstrated considerable functions similar to those of Pyr3 or 2-aminoethyl diphenylborinate inhibitors and suppressed high glucose-induced effects, including the blockade of transient receptor potential (TRP) cation channel subfamily C member 3 (TRPC3) and TRPC6 protein expression and decreases in ROS and inducible nitric oxide synthase expression (16). Based on the determinant role of 18 $\beta$ -GA in inhibiting ROS generation and inflammatory infiltration, it was hypothesized that 18 $\beta$ -GA protects against nerve injury caused by hydrogen peroxide (H<sub>2</sub>O<sub>2</sub>). However, the mechanism of the neuroprotective effect of 18 $\beta$ -GA has so far remained elusive.

Network pharmacology has illustrated the synergistic effects and underlying mechanisms of herbs via network analysis, which is an appropriate way to measure the effectiveness and demonstrate the functional mechanisms of novel bioactive compounds. In the present study, network pharmacology was applied to identify related targets of 18 $\beta$ -GA for the treatment of neuronal injury and these targets were then experimentally verified. This experimental verification suggested that 18 $\beta$ -GA protected Schwann cells from H<sub>2</sub>O<sub>2</sub>-induced injury by inhibiting the phosphorylation of p38 MAPK.

## Methods

**Pathway prediction based on network pharmacology.** The SMILES annotation for the drug 18 $\beta$ -GA was found in PubChem. After searching Swiss Target Prediction, the Similarity Ensemble Approach (SEA) Search Server and TargetNet (<http://www.swisstargetprediction.ch>, <http://sea.bkslab.org> and <http://targetnet.scbdd.com/home/index>, respectively), SMILES for monomer drugs was selected and the species was limited to *Homo sapiens*. The obtained protein targets and corresponding UniProt IDs were imported into Excel. By entering the keywords 'injury', 'damage' and 'harm' into the 'GeneCards database' (<https://www.genecards.org>), reported injury-related genes were acquired. The common targets of injury and 18 $\beta$ -GA were screened by Wayne diagram analysis. These targets were imported into the WebGestalt database (<http://www.webgestalt.org/>) and Kyoto Encyclopedia of Genes and Genomes (KEGG; [https://www.genome.jp/dbget-bin/www\\_bget?pathway:map04750](https://www.genome.jp/dbget-bin/www_bget?pathway:map04750)) pathway analysis was performed with  $P < 0.05$  and gene count  $\geq 5$ .

**Reagents and cell line.** 18 $\beta$ -GA (cat. no. G109796; 98.0%) was acquired from Shanghai Aladdin Biochemical Technology Co., Ltd. PBS, Triton X, TBS and neutral balsam were purchased from Shuyan Biological Technology Co., Ltd. Trypsin was acquired from Guangzhou Saiguo Biological Co., Ltd. PageR $\mu$ Ler Prestained Protein Ladder and Marker (cat. no. P12083) were obtained from Shanghai Bioscience Technology Co. Ltd. SB203580 (a p38 MAPK inhibitor) was purchased from Selleck Chemicals. Polyvinylidene difluoride (PVDF) membranes were obtained from MilliporeSigma. Hoechst 33258 stain (cat. no. RYS580), phosphatase inhibitor cocktail 1 (cat. no. RBG2012) and a BCA protein content kit (cat. no. P0010S) were acquired from Guangzhou Junji Biotechnology Co., Ltd. RIPA buffer (cat. no. WB-0071) was purchased from Beijing Dingguo Biological Co., Ltd. Rabbit antibodies against TRP vanilloid 1 (TRPV1), TRP ankyrin 1 (TRPA1),  $\beta$ -actin, cleaved-caspase-3, cleaved-caspase-7, Bcl-xL, p38 MAPK, phosphorylated (p)-p38 MAPK, Bcl-2, Bax and Bad (cat. nos. ab6166, NB110-40763, 9662S, 9664S, 8438S, 2764S, 8690S, 4511S, ab117115, 2772 and 9292, respectively) were acquired from Guangzhou Juyan Biological Co., Ltd. Goat anti-rabbit secondary antibody (cat. no. CW0103) was acquired from Guangzhou Juyan Biological Co., Ltd. Meilunbio<sup>®</sup> ECL reagent (cat. no. MA0186-100ML) was acquired by Guangzhou Jiayan Biological Co., Ltd. A Cell Counting Kit-8 (CCK-8; cat. no. 96992) was acquired from Sigma-Aldrich (Merck KGaA). The Annexin V FITC Apoptosis Detection Kit I (cat. no. 556547) was obtained from Guangzhou Juyan Biological Co., Ltd. Diluted primary antibody, diluted secondary antibody, western blot transfer solution and western blot electrophoresis solution were obtained from Servicebio. RNAiso Plus was acquired from Takara Biotechnology, Co., Ltd. SYBR<sup>®</sup>-Green Premix qPCR, an Evo M-MLV RT-PCR kit and RNase-free water (cat. nos. AG11701, AG11602 and AG11012) were obtained from Accurate Biotechnology Co., Ltd. The Schwann cell line RSC96 was acquired from Shanghai Institute of Cell (cat. no. GNR6). The cell line used in the experiments was between passages 8 and 13.

**Cell viability and cytotoxicity assays.** The viability of Schwann cells was determined by the CCK-8 assay. First, Schwann cells were seeded into 96-well plates at a density of  $6 \times 10^3$  cells/well for 24 h. To assess H<sub>2</sub>O<sub>2</sub>-induced injury, cells were incubated with H<sub>2</sub>O<sub>2</sub> at various concentrations (0, 20, 50, 100, 150, 200, 250 and 300  $\mu$ M) for 4 h and then subjected to the CCK-8 assay. For the 18 $\beta$ -GA-mediated protection assay, Schwann cells were pre-treated with 18 $\beta$ -GA (0, 2.5, 5, 7.5, 10, 15, 20 and 30  $\mu$ M) 24 h prior to being exposed to H<sub>2</sub>O<sub>2</sub> (200  $\mu$ M) for 4 h. After the incubation, the medium was discarded and the cells were then incubated with CCK-8 solution at 37°C for 1 h. The absorbance (450 nm) was then measured by using a microplate reader (Bio-Tek Instruments, Inc.).

**Experimental grouping.** The experimental groups were as follows: Control, model (200  $\mu$ M H<sub>2</sub>O<sub>2</sub>), 10  $\mu$ M SB203580 (200  $\mu$ M H<sub>2</sub>O<sub>2</sub> + 10  $\mu$ M SB203580), 5  $\mu$ M GA (H<sub>2</sub>O<sub>2</sub> 200  $\mu$ M + 5  $\mu$ M 18 $\beta$ -GA; GA5) and 10  $\mu$ M GA (200  $\mu$ M H<sub>2</sub>O<sub>2</sub> + 10  $\mu$ M 18 $\beta$ -GA; GA10) groups. In brief, Schwann cells ( $1.2 \times 10^5$  cells/well) were cultivated in 6-well plates. The medium

Table I. Primer sequences used for PCR.

Gene	Forward primer (5'-3')	Reverse primer (5'-3')
TRPA1	AAATGCCACAGTTCTCAA	TCTTCGTGTTGCCCTTAT
TRPV1	TTCAAGGGTTCCACGAGA	AGTGCCGACACCTATCCA
TNF- $\alpha$	GCGTGTTTCATCCGTTCTCTACC	TACTTCAGCGTCTCGTGTGTTTCT
IL-1 $\beta$	AGGAGAGACAAGCAACGACA	CTTTTCCATCTTCTTTTGGGTAT
$\beta$ -actin	GAGAGGGAAATCGTGCGT	GGAGGAAGAGGATGCGG

TRPA1, transient receptor potential ankyrin 1; TRPV1, transient receptor potential vanilloid 1.

was then discarded and the cells were washed with PBS. The cells were then incubated with 18 $\beta$ -GA at 5 or 10  $\mu$ M concentrations or SB203580 for 24 h. After the medium was discarded, the cells were washed with PBS and they were incubated with 200  $\mu$ M H<sub>2</sub>O<sub>2</sub> (dissolved in PBS) for 4 h at 37°C.

**Intracellular ROS measurement.** An intracellular ROS measurement assay was performed as previously described (17). After being cultivated for 24 h, Schwann cells were incubated at 37°C for 20 min in PBS containing 20  $\mu$ M 2',7'-dichlorodihydrofluorescein diacetate (DCFH-DA). Subsequently, the cells were treated with 18 $\beta$ -GA at two fixed concentrations or SB203580 and then incubated with 200  $\mu$ M H<sub>2</sub>O<sub>2</sub> in PBS. After the PBS had been removed, intracellular ROS production was measured on an inverted fluorescence microscope. Photomicrographs of three fields were taken for each well. The amount of intracellular ROS was determined based on the fluorescence intensity via Image-Pro Plus 6.0 (Media Cybernetics, Inc.).

**Hoechst 33258 staining.** After pre-treatment and incubation with 200  $\mu$ M H<sub>2</sub>O<sub>2</sub> in PBS at 37°C for 4 h, cells were incubated with Hoechst 33258 (5  $\mu$ l in 1.0 ml of PBS) in each well for 20 min. After washing twice with PBS, fluorescence images were acquired using an inverted fluorescence microscope. Three photomicrographs were captured per well, and Image-Pro Plus 6.0 was used for analysis.

**Cell apoptosis detection via flow cytometry.** Annexin V FITC and propidium iodide (PI) were used to evaluate the apoptotic rates of Schwann cells in different groups. After pre-treatment, cells were incubated with 200  $\mu$ M H<sub>2</sub>O<sub>2</sub> in PBS at 37°C for 4 h. Cells were collected with trypsin and washed with PBS. Subsequently, 1x10<sup>6</sup> cells were placed in binding buffer and double-stained with Annexin V FITC and PI in the dark for 15 min at 4°C. The proportion of early + late apoptotic cells was then analysed on a flow cytometer (CytExpert 2.3; Beckman Coulter, Inc.) to determine the apoptotic rate.

**Reverse-transcription quantitative (RT-qPCR).** According to the manufacturer's protocol, total RNA was isolated using RNAiso Plus. Subsequently, cDNA was synthesized based on the instructions of the RT-PCR kit. Then, a Bio-Rad CFX96 Real-Time PCR System (Bio-Rad Laboratories, Inc.) was used to perform qPCR. The amplification parameters were 95°C for 30 sec, followed by 40 cycles of 95°C for 5 sec and

60°C for 34 sec, 95°C for 15 sec, 60°C for 60 sec and 95°C for 15 sec. The relative expression of mRNA was calculated by the 2<sup>- $\Delta\Delta$ C<sub>q</sub></sup> method (18) after normalization to  $\beta$ -actin. For this procedure, SYBR<sup>®</sup>-Green Premix qPCR and primers (Table I) were used.

**Western blot analysis.** Changes in the expression of Bcl-x1, Bcl-2, Bad, Bax, cleaved-caspase 3 and cleaved-caspase 7, which are related to apoptosis pathways, were assessed by western blot analysis. The levels of TRPA1 and TRPV1, which are closely related to injury, were also measured. RIPA buffer was used to lyse the cells and obtain the proteins from the supernatant. The protein concentration was determined via a BCA assay, and samples (30  $\mu$ g) were separated via 4-10% SDS-PAGE followed by transfer to PVDF membranes and blocking with 5% skim milk at 37°C for 1 h. PVDF membranes were incubated with primary antibody (1:1,000 dilution) overnight at 4°C for 24 h and then with secondary antibody (1:5,000 dilution) for 45 min at 37°C. Finally, chemiluminescence was used to visualize the bands for assessment of the images via Image-Lab 3.0 (Bio-Rad Laboratories, Inc.).

**Statistical analyses.** Values are expressed as the mean  $\pm$  standard deviation. Experiments were repeated three times. GraphPad Prism 8 (GraphPad Software, Inc.) and SPSS 13.0 (SPSS, Inc.) software were used to perform statistical analysis. The data were analyzed by one-way ANOVA. Bonferroni's test was the post hoc test after ANOVA. P<0.05 was considered to indicate a statistically significant difference.

## Results

**Target of 18 $\beta$ -GA activity.** Through PubChem, the SMILES annotation for 18 $\beta$ -GA was obtained, which is 'CC1(C2CCC3(C(C2(CCC1O)C)C(=O)C=C4C3(CCC5(C4CC(C5)C)C(=O)O)C)C)C'. This sequence was inputted into Swiss Target Prediction, the SEA Search Server and TargetNet, which identified 126 active targets. In addition, 15,327 targets associated with injury were identified. A total of 111 potential targets associated with 18 $\beta$ -GA for injury management were further identified. Targets of 18 $\beta$ -GA with potential for injury treatment were inputted into the STRING database along with the species. The top 10 pathways were ranked and are presented in Fig. 1. In a previous experiment, it was indicated that model rats with chronic constriction injury of the sciatic nerve exhibited increased inflammation (19).

Therefore, ‘Inflammatory mediator regulation of TRP channels’, was chosen for experimental verification.

**Effects of H<sub>2</sub>O<sub>2</sub> and 18 $\beta$ -GA on Schwann cell viability.** H<sub>2</sub>O<sub>2</sub> decreased cell viability in a concentration-dependent manner. A moderate response (~50%) was induced by 200  $\mu$ M H<sub>2</sub>O<sub>2</sub> (Fig. 2A). To examine the cytotoxicity of 18 $\beta$ -GA, Schwann cells were incubated with various doses of 18 $\beta$ -GA at 37°C for 24 h. Cytotoxicity was determined based on the results of the CCK-8 assays. Treatment with 10  $\mu$ M 18 $\beta$ -GA significantly increased cell viability ( $P < 0.05$ ; Fig. 2B), confirming that a suitable concentration had been used. The concentrations of 10 and 5  $\mu$ M were subsequently applied to achieve a dose-effect relationship and it was more suitable to choose 5  $\mu$ M than 7.5  $\mu$ M 18 $\beta$ -GA.

**18 $\beta$ -GA inhibits H<sub>2</sub>O<sub>2</sub>-induced ROS production in Schwann cells.** To determine whether the cytoprotective effects of 18 $\beta$ -GA are an intracellular effect, it was investigated whether 18 $\beta$ -GA is able to be transported into Schwann cells to inhibit H<sub>2</sub>O<sub>2</sub>-induced intracellular radical production. In brief, cells were first stressed with 18 $\beta$ -GA; 20  $\mu$ M DCFH-DA was then added before intracellular ROS levels were evaluated. In this way, as 18 $\beta$ -GA and H<sub>2</sub>O<sub>2</sub> did not come into contact in the extracellular space, any reduction in ROS levels was attributed to an intracellular effect. Treatment of Schwann cells with H<sub>2</sub>O<sub>2</sub> increased intracellular ROS levels compared with those of untreated cells. However, 18 $\beta$ -GA and SB203580 attenuated ROS accumulation. The difference in ROS production under treatment with 200  $\mu$ M H<sub>2</sub>O<sub>2</sub> with and without 18 $\beta$ -GA was significant (Fig. 3). These results indicated that 18 $\beta$ -GA and SB203850 are able to decrease H<sub>2</sub>O<sub>2</sub>-induced ROS production in Schwann cells.

**Hoechst 33258 staining.** To determine whether 18 $\beta$ -GA protects the nucleus from damage, nuclei were subjected to Hoechst 33258 staining. After H<sub>2</sub>O<sub>2</sub> treatment, Schwann cells exhibited apoptotic nuclei, but pre-treatment with 18 $\beta$ -GA and SB203580 markedly abrogated these effects. 18 $\beta$ -GA and SB203580 inhibited the formation of apoptotic nuclei induced by H<sub>2</sub>O<sub>2</sub> treatment (Fig. 4).

**Flow cytometry results.** Flow cytometry was performed to investigate whether 18 $\beta$ -GA protects Schwann cells against H<sub>2</sub>O<sub>2</sub>-induced apoptosis (Fig. 5). The proportion of apoptotic cells was obviously lower in the control group ( $4.34 \pm 0.27\%$ ) than in the model group ( $12.63 \pm 1.21\%$ ). In addition, the percentage of apoptotic cells was markedly lower in the group pre-treated with SB203580 or 5 or 10  $\mu$ M 18 $\beta$ -GA ( $7.02 \pm 0.30$ ,  $4.83 \pm 0.55$  and  $4.88 \pm 0.50\%$ , respectively) than in the model group ( $P < 0.05$ ). 18 $\beta$ -GA enabled the recovery of cell viability to its normal level. These results suggested that 18 $\beta$ -GA and SB203580 markedly inhibited H<sub>2</sub>O<sub>2</sub>-induced apoptosis.

**mRNA levels of TRPA1, TRPV1, IL1 $\beta$  and TNF- $\alpha$ .** To explore the mRNA expression of TRPV1, TRPA1, IL-1 $\beta$  and TNF- $\alpha$ , RT-qPCR analysis was applied (Fig. 6). The mRNA expression of TRPV1, TRPA1, IL-1 $\beta$  and TNF- $\alpha$  in the control group was evidently enhanced after treatment with H<sub>2</sub>O<sub>2</sub> ( $P < 0.05$ ). By contrast, 18 $\beta$ -GA decreased the expression of these genes

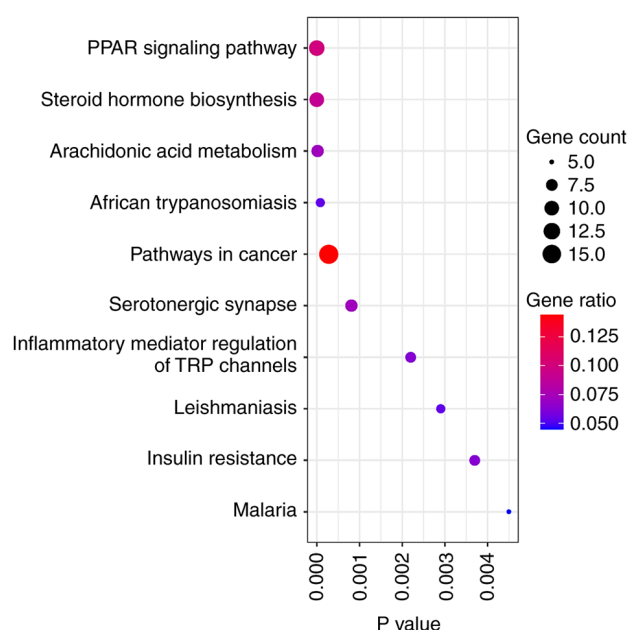


Figure 1. KEGG pathway analysis of target genes of 18 $\beta$ -GA. KEGG pathway enrichment analysis of 18 $\beta$ -GA targets with potential for treating damage was performed via DAVID. The top 10 pathways were ranked. KEGG, Kyoto Encyclopedia of Genes and Genomes; 18 $\beta$ -GA, 18 $\beta$ -glycyrrhetic acid.

( $P < 0.05$ ). The mRNA levels of the four genes returned to normal in the groups treated with SB203580 or 5 or 10  $\mu$ M 18 $\beta$ -GA. Thus, 18 $\beta$ -GA had an anti-inflammatory effect.

**Expression of TRP, apoptotic, antiapoptotic and p38 MAPK proteins.** Western blot analysis was used to determine the expression of various proteins (Fig. 7). H<sub>2</sub>O<sub>2</sub> decreased the expression of Bcl-2 and Bcl-x1 ( $P < 0.05$ ), which are antiapoptotic proteins, while pre-treatment with 18 $\beta$ -GA abrogated the effect ( $P < 0.05$ ). Furthermore, H<sub>2</sub>O<sub>2</sub> was indicated to increase the expression of Bax, Bad, cleaved-caspase-3 and cleaved-caspase-7 ( $P < 0.05$ ), which are proapoptotic proteins. Of note, in comparison to the H<sub>2</sub>O<sub>2</sub>-treated model group, SB203580 and 18 $\beta$ -GA enhanced the levels of Bcl-2 and Bcl-x1, and decreased the Bax, Bad, cleaved-caspase-3 and cleaved-caspase-7 levels ( $P < 0.05$ ), which were nearly normal.

The levels of TRPV1, TRPA1 and p-p38 MAPK in the model group were clearly increased after treatment with H<sub>2</sub>O<sub>2</sub> ( $P < 0.05$ ). However, the p38 MAPK levels did not vary among the groups. 18 $\beta$ -GA and SB203580 reduced the expression of the three proteins compared with those in the model group ( $P < 0.05$ ). Furthermore, 18 $\beta$ -GA decreased TRPA1 to near-normal levels. However, SB203580 only slightly decreased the levels of TRPA1 and they remained significantly higher than those in the control group ( $P < 0.05$ ). Overall, the inhibitory effects of 18 $\beta$ -GA and SB203580 at different concentrations were similar, suggesting that 18 $\beta$ -GA was able to suppress the activation of p38 MAPK and the protein levels of TRPA1 and TRPV1.

## Discussion

For network pharmacology research, the top 10 KEGG pathways are typically selected. In the present study, the pathway

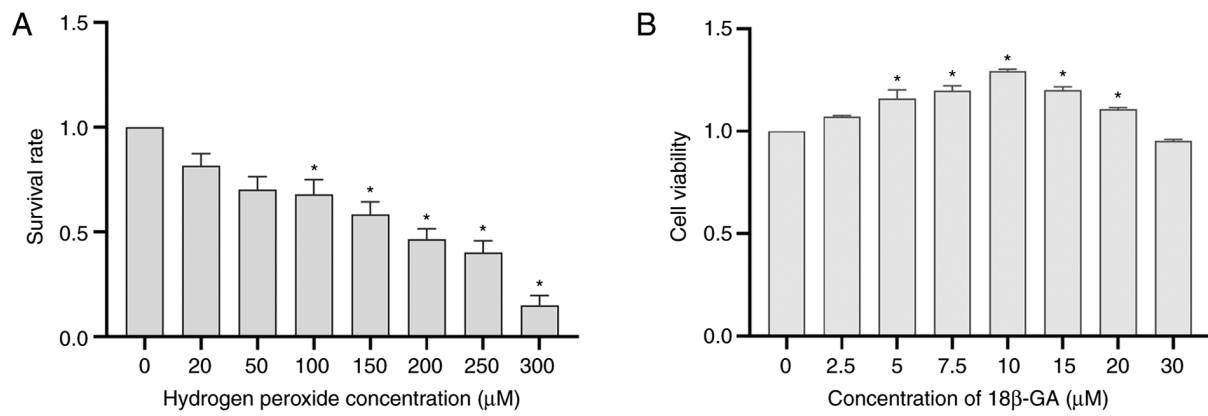


Figure 2. Cell viability and cytotoxicity assay. (A)  $H_2O_2$  decreased cell viability in a concentration-dependent manner. (B) 18β-GA affected Schwann cell viability. \* $P < 0.05$  vs. control (0 μM  $H_2O_2$  or 18β-GA). 18β-GA, 18β-glycyrrhetic acid.

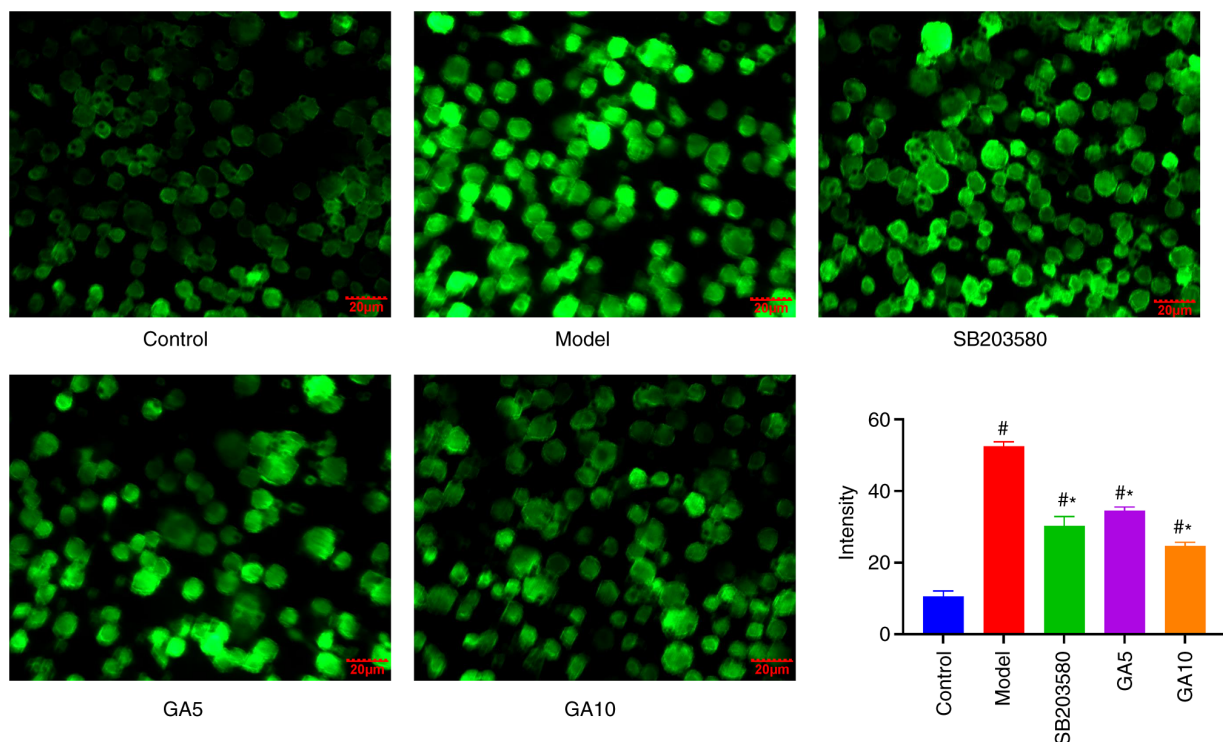


Figure 3. 18β-GA inhibits  $H_2O_2$ -induced ROS production.  $H_2O_2$ , 18β-GA and SB203580 affected the levels of intracellular ROS (scale bar, 20 μm). # $P < 0.05$  vs. control group; \* $P < 0.05$  vs. model group. 18β-GA, 18β-glycyrrhetic acid; ROS, reactive oxygen species; GA5, 5 μM 18β-GA; GA10, 10 μM 18β-GA. ROS, reactive oxygen species.

'Inflammatory mediator regulation of TRP channels' was selected, which contains IL-1β, phospholipase Cγ1 (PLCG1), protein kinase Cα (PRKCA), PRKCH, prostaglandin E receptor 2 (PTGER2), PTGER4 and TRPA1, for experimental verification. The experiments of the present study demonstrated that  $H_2O_2$  induced oxidative stress and increased the proportion of apoptotic nuclei and the apoptotic rate in Schwann cells.  $H_2O_2$  increased intracellular ROS and the levels of Bax, Bad, cleaved-caspase-3 and cleaved-caspase-7, while decreasing the levels of Bcl-2, Bcl-x1, TRPA1 and TRPV1 and p-p38 MAPK. In addition,  $H_2O_2$  exposure increased the mRNA levels of TRPA1, TRPV1, IL-1β and TNF-α. However, pre-treatment with 18β-GA and SB203580 notably decreased the level of ROS and particularly prevented

nuclear and Schwann cell apoptosis. In addition, pre-treatment with 18β-GA and SB203580 clearly reduced the protein levels of Bax, Bad, cleaved-caspase-3, cleaved-caspase-7, TRPA1, TRPV1 and p-p38 MAPK and the mRNA levels of TRPA1, TRPV1, IL-1β and TNF-α, and enhanced the levels of Bcl-x1 and Bcl-2 in comparison with the model group.

Regarding the inflammatory pathway by which TRP channels are regulated, IL-1β, PLCG1, PRKCA, PRKCH, PTGER2 and PTGER4 are the upstream targets of TRPA1, as indicated in a signalling pathway on the official KEGG website (pathway map: map04750). Through this pathway of inflammation-mediated regulation of TRP channels, the expression of TRPA1 may be regulated by the p38 signalling pathway. Indeed, TRPA1 and TRPV1 are generally co-expressed in

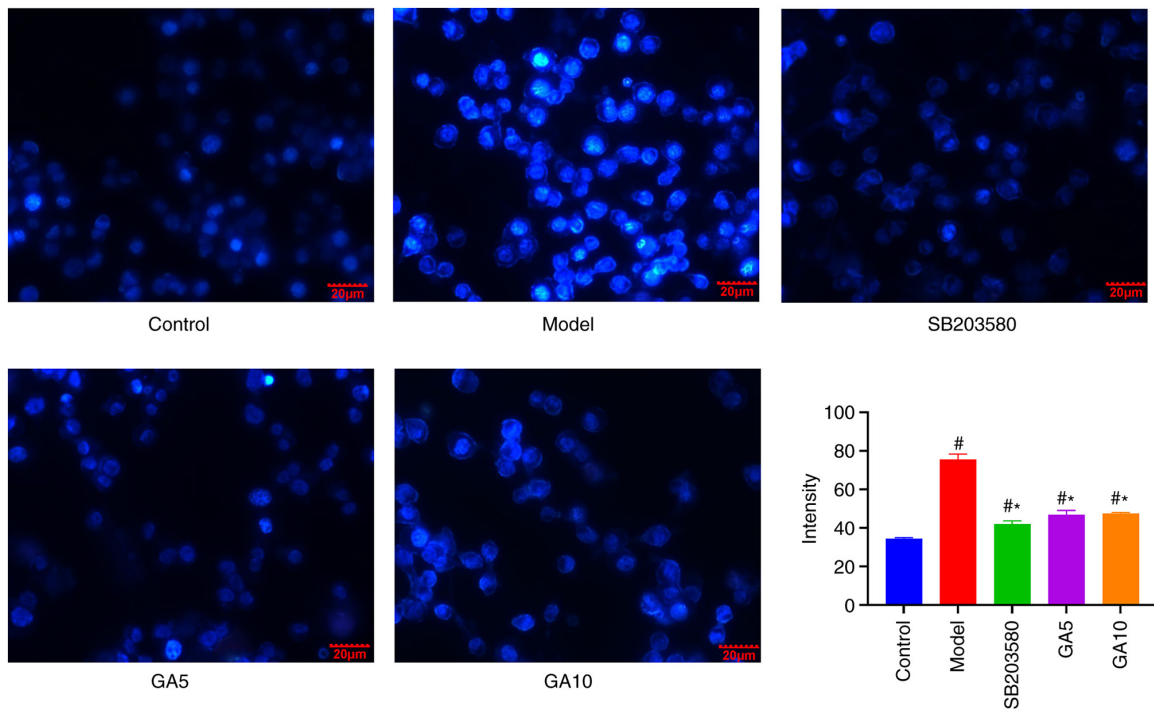


Figure 4. 18 $\beta$ -GA reverses H<sub>2</sub>O<sub>2</sub>-induced changes in condensed chromatin and apoptotic nuclei. H<sub>2</sub>O<sub>2</sub>, 18 $\beta$ -GA and SB203580 affected changes in the nuclei (scale bar, 20  $\mu$ m). <sup>#</sup>P<0.05 vs. control group; <sup>\*</sup>P<0.05 vs. model group. 18 $\beta$ -GA, 18 $\beta$ -glycyrrhethinic acid; GA5, 5  $\mu$ M 18 $\beta$ -GA; GA10, 10  $\mu$ M 18 $\beta$ -GA.

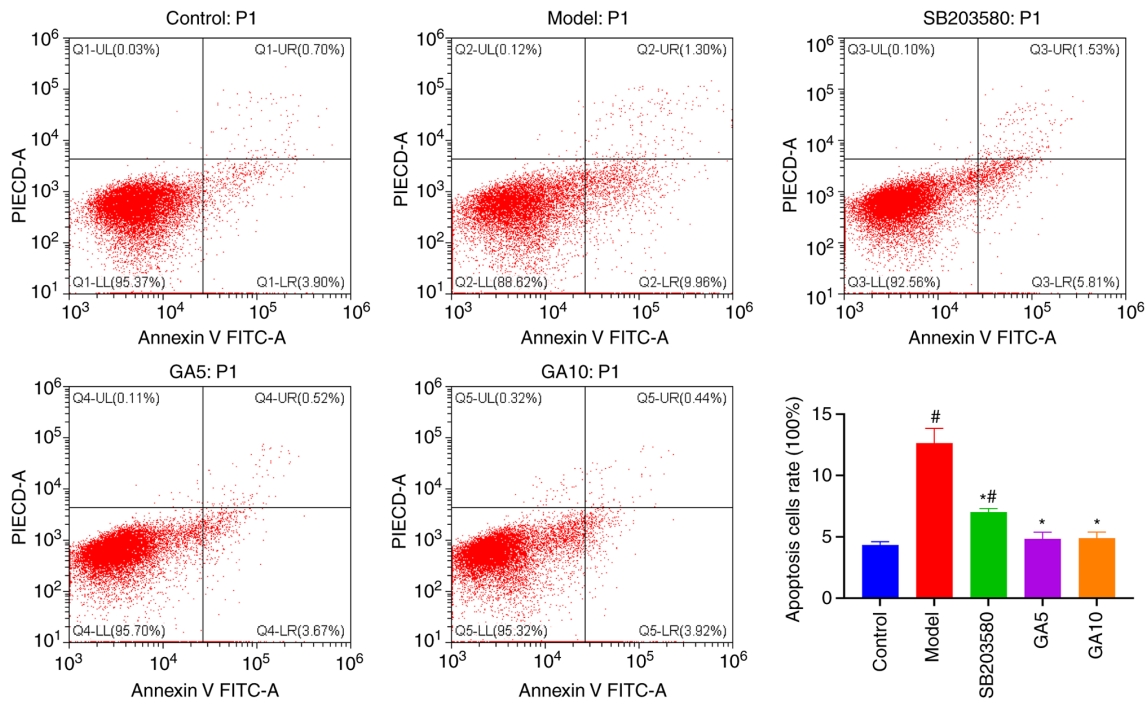


Figure 5. Protective effect of 18 $\beta$ -GA against H<sub>2</sub>O<sub>2</sub>-induced apoptosis. Flow cytometry revealed that H<sub>2</sub>O<sub>2</sub>, 18 $\beta$ -GA and SB203580 affected the levels of cell apoptosis. <sup>#</sup>P<0.05 vs. control group; <sup>\*</sup>P<0.05 vs. model group. 18 $\beta$ -GA, 18 $\beta$ -glycyrrhethinic acid; PI, propidium iodide; Q, quadrant; UL, upper left; UR, upper right; LL, lower left; LR, lower right; GA5, 5  $\mu$ M 18 $\beta$ -GA; GA10, 10  $\mu$ M 18 $\beta$ -GA.

cells (20). Therefore, TRPA1, TRPV1 and p38 MAPK were selected as proteins from the inflammation-mediated regulation of the TRP channel pathway for analysis in the present study. According to differences in the expression levels determined by PCR and western blot analysis, a p38 inhibitor (SB203580) attenuated the H<sub>2</sub>O<sub>2</sub>-induced increase in TRPA1,

TRPV1 and p-p38 MAPK at the protein level. These results suggested that TRPA1 and TRPV1 are related to injury and apoptosis. Furthermore, TRPA1 and TRPV1 were indicated to mediate cigarette smoke extract-induced damage by regulating oxidative stress, inflammatory infiltration and mitochondrial injury in bronchial epithelial cells (21).

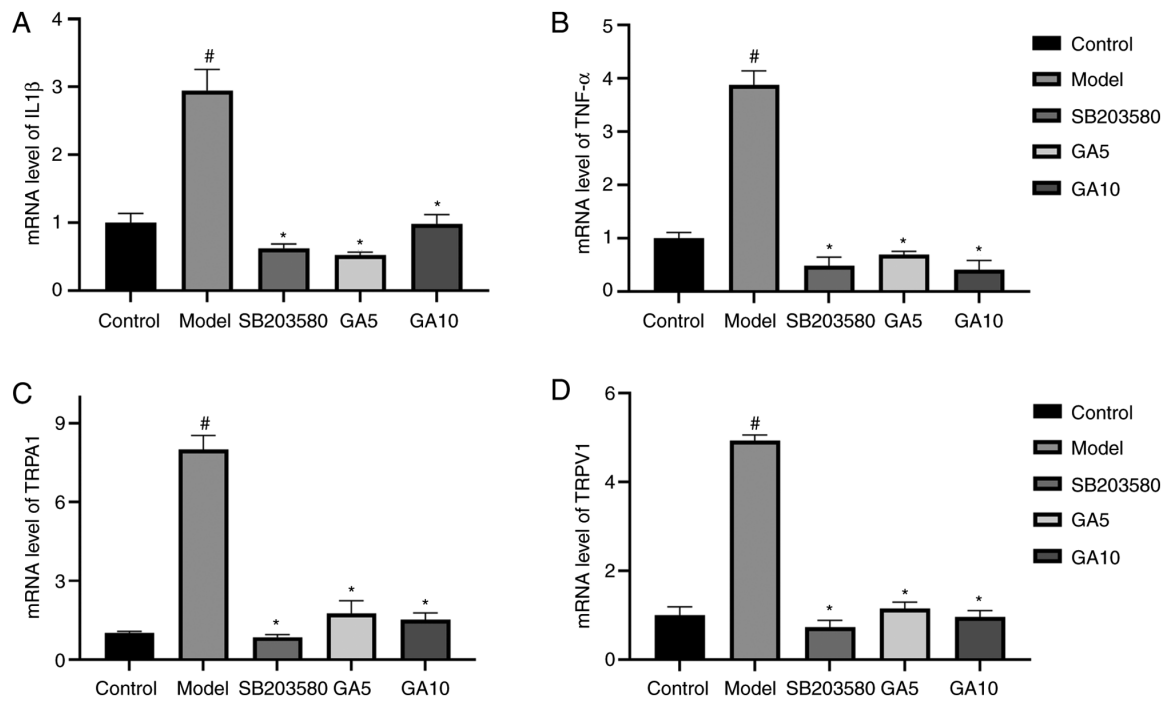


Figure 6. mRNA analysis of inflammatory markers. mRNA levels of (A) IL-1 $\beta$ , (B) TNF- $\alpha$ , (C) TRPA1 and (D) TRPV1 in the different groups determined by reverse transcription-quantitative PCR. \*P<0.05 vs. control group; #P<0.05 vs. model group. 18 $\beta$ -GA, 18 $\beta$ -glycyrrhetic acid; TRPA1, transient receptor potential ankyrin 1; TRPV1, transient receptor potential vanilloid 1; GA5, 5  $\mu$ M 18 $\beta$ -GA; GA10, 10  $\mu$ M 18 $\beta$ -GA.

Oxidative stress is involved in injury and apoptosis. The accumulation of ROS may result in various forms of oxidative protein, lipid and DNA modifications, leading to cellular damage. 18 $\beta$ -GA pre-treatment strongly regulated these oxidative conditions, and 18 $\beta$ -GA and SB203580 attenuated ROS accumulation. Previous studies demonstrated that Bcl-x1 and Bcl-2 were associated with apoptosis induced by ROS accumulation (22); furthermore, ROS activate caspase-3 (22). Su *et al* (3) determined that 18 $\beta$ -GA treatment decreased the accumulation of ROS in RAW264.7 cells after exposure to X-ray radiation. SB203580 decreased the expression of cleaved-caspase 3 reduced the level of cleaved-caspase 7. SB203580 increased the expression of Bcl-x1 and Bcl-2 after H<sub>2</sub>O<sub>2</sub> treatment. In addition, the proportion of apoptotic cells was obviously lower in the group pre-treated with SB203580 than in the group pre-treated with H<sub>2</sub>O<sub>2</sub> alone. Similarly, SB203580 reversed the increase in condensed chromatin and apoptotic nuclei after treatment with H<sub>2</sub>O<sub>2</sub>. Initial reports have suggested that p38 MAPK regulates mitochondria in drug-induced cancer cell apoptosis (23). These results are in agreement with the generally accepted knowledge that the inhibition of p38 MAPK phosphorylation prevents apoptosis (24). The p38 MAPK inhibitor SB202190 reduced TNF- $\alpha$ -induced TRPA1 expression.

Coskun *et al* (25) indicated that TNF- $\alpha$  induced tissue damage mediated by neutrophils. After treatment with H<sub>2</sub>O<sub>2</sub>, the mRNA levels of IL-1 $\beta$  and TNF- $\alpha$  increased sharply. Pre-treatment with 18 $\beta$ -GA reversed this trend. Previously, 18 $\beta$ -GA was reported to significantly inhibit lipopolysaccharide-induced TNF- $\alpha$  production (26). Ishida *et al* (27) indicated that the binding of hydroxypropyl- $\gamma$ -cyclodextrin and 18 $\beta$ -GA had a negative effect on IL-6, IL-1 $\beta$ , TNF- $\alpha$  and mRNA expression and enhanced intestinal injury induced by

indomethacin. Furthermore, Su *et al* (3) reported that 18 $\beta$ -GA inhibited radiation-induced inflammation by decreasing the accumulation of inflammatory cytokines, including IL-6 and IL-1 $\beta$ , caused by radiation. The results in the present study are similar to those of the aforementioned studies. Therefore, 18 $\beta$ -GA is able to attenuate the mRNA expression of TNF- $\alpha$  and IL-1 $\beta$ , which may reduce the degree of cell apoptosis.

18 $\beta$ -GA increased the expression of Bcl-x1 and Bcl-2 after H<sub>2</sub>O<sub>2</sub> treatment and decreased the expression of Bax, Bad, cleaved-caspase-3 and cleaved-caspase-7. In addition, the proportion of apoptotic cells was notably higher in the group treated with H<sub>2</sub>O<sub>2</sub> alone than in the group pre-treated with 18 $\beta$ -GA. 18 $\beta$ -GA similarly inhibited the protein levels of p-p38 MAPK. Su *et al* (3) indicated that 18 $\beta$ -GA exhibited anti-inflammatory activity against radiation-induced skin damage by inhibiting ROS accumulation and restricting the activation of the NF- $\kappa$ B and p38 MAPK pathways. The present results suggested that 18 $\beta$ -GA prevented Schwann cell injury and apoptosis induced by H<sub>2</sub>O<sub>2</sub> via the p38 MAPK pathway.

There was no significant difference between 5 and 10  $\mu$ M 18 $\beta$ -GA in terms of their anti-apoptosis effect and regulation of various signaling factors. These two concentrations were selected with the aim of obtaining a dose-effect relationship, but this was not achieved. A CCK-8 assay was used to detect cell viability. However, whilst this experiment indicates the toxicity of 18 $\beta$ -GA to cells, it may not reveal anti-damage effects of a compound; this may be the reason why the two concentrations of 18 $\beta$ -GA had the same effect.

The typical manifestations of peripheral nerve injury are increased oxidative stress (28,29), cell damage (28) and inflammatory infiltration (30). It was indicated that 18 $\beta$ -GA was able to alleviate these effects by decreasing inflammatory

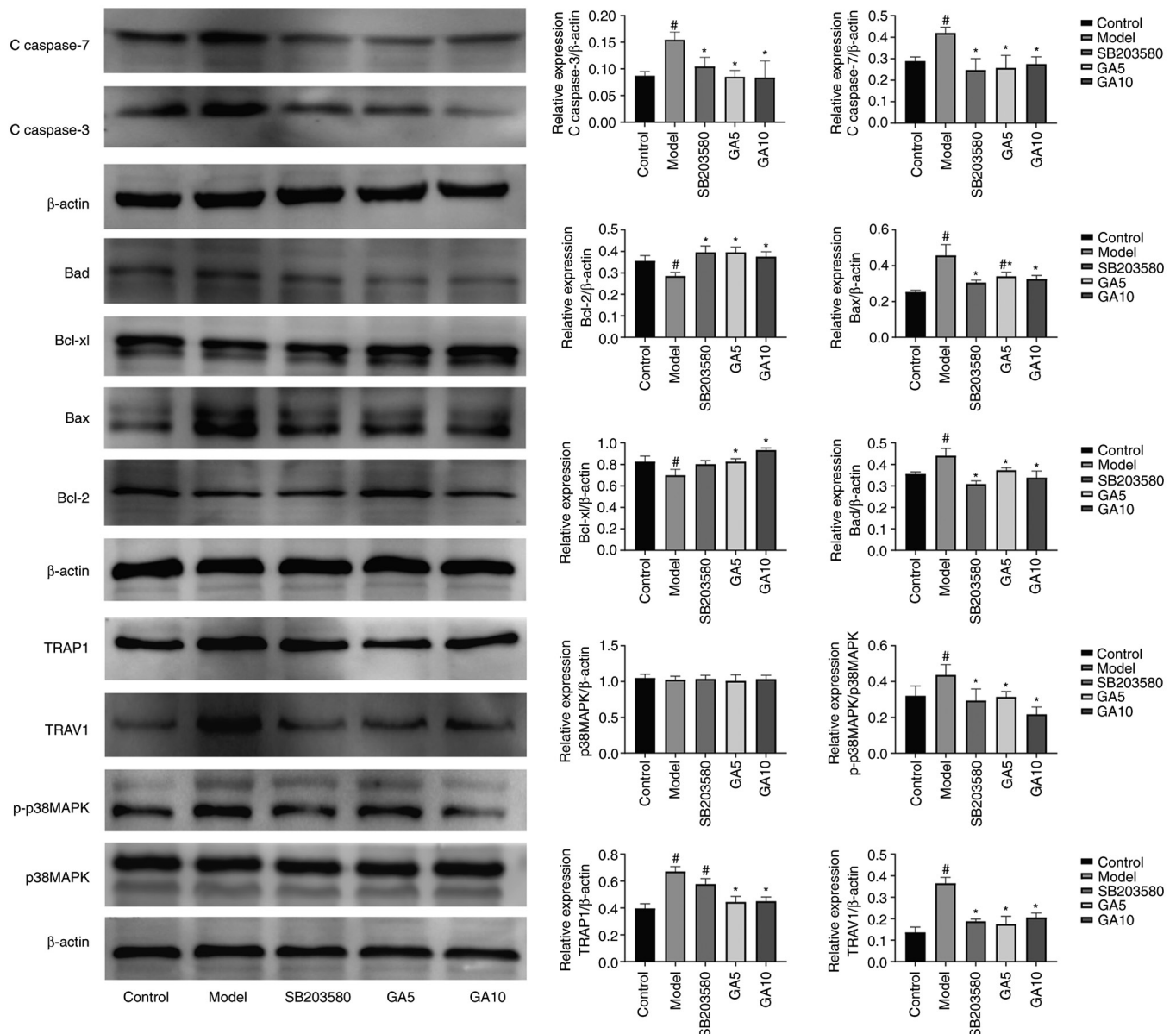


Figure 7. Expression of TRP, apoptotic, antiapoptotic and p38 MAPK proteins in different groups determined by western blot analysis. #P<0.05 vs. control group; \*P<0.05 vs. model group. 18 $\beta$ -GA, 18 $\beta$ -glycyrrhetic acid; TRPA1, transient receptor potential ankyrin 1; TRPV1, transient receptor potential vanilloid 1; p-p38, phosphorylated p38; GA5, 5  $\mu$ M 18 $\beta$ -GA; GA10, 10  $\mu$ M 18 $\beta$ -GA.

factors, decreasing the elevated expression of TRP proteins and inhibiting p38 MAPK phosphorylation.

However, there were limitations to the present *in vitro* experiments. Cell experiments are able to demonstrate that a drug has therapeutic potential for peripheral nerve injury prior to animal experiments. However, the main disadvantage of *in vitro* experimental research is that it is challenging to extrapolate the results to the biology of intact organisms, as the body is not a single-celled organism.

In conclusion, H<sub>2</sub>O<sub>2</sub> increased intracellular ROS and the levels of Bax, Bad, cleaved-caspase-3 and cleaved-caspase-7 and decreased the levels of Bcl-xl and Bcl-2. Furthermore, H<sub>2</sub>O<sub>2</sub> exposure increased the protein levels of TRPA1 and TRPV1 and the phosphorylation of p38 MAPK. 18 $\beta$ -GA and SB203580 attenuated ROS accumulation, inhibited the phosphorylation of p38 MAPK, enhanced the expression of Bcl-xl and Bcl-2 and decreased the levels of cleaved-caspase-7,

cleaved-caspase-3, Bax and Bad, which indicated that 18 $\beta$ -GA may be a candidate drug to prevent peripheral nerve injury.

## Acknowledgements

Not applicable.

## Funding

This work was supported by the National Natural Science Foundation of China (grant no. 81874404).

## Availability of data and materials

The datasets used and/or analyzed during the current study are available from the corresponding author on reasonable request.

## Authors' contributions

DZ, JS, SC and GZ made considerable contributions to the experimental design, statistical data analysis and experimental procedures. XL, HS, BJ, YZ, YL, GQ and YP assisted with the English writing, and made substantial contributions towards the experimental design and statistical analysis. DZ and JS checked and confirmed the authenticity of the raw data. All authors read and approved the final manuscript.

## Ethics approval and consent to participate

Not applicable.

## Patient consent for publication

Not applicable.

## Competing interests

The authors declare that they have no competing interests.

## References

- Pastorino G, Cornara L, Soares S, Rodrigues F and Oliveira MBPP: Liquorice (*Glycyrrhiza glabra*): A phytochemical and pharmacological review. *Phytother Res* 32: 2323-2339, 2018.
- Abd El-Twab SM, Hozayen WG, Hussein OE and Mahmoud AM: 18 $\beta$ -glycyrrhetic acid protects against methotrexate-induced kidney injury by up-regulating the Nrf2/ARE/HO-1 pathway and endogenous antioxidants. *Ren Fail* 38: 1516-1527, 2016.
- Su L, Wang Z, Huang F, Lan R, Chen X, Han D, Zhang L, Zhang W and Hong J: 18 $\beta$ -glycyrrhetic acid mitigates radiation-induced skin damage via NADPH oxidase/ROS/p38MAPK and NF- $\kappa$ B pathways. *Environ Toxicol Pharmacol* 60: 82-90, 2018.
- Mahmoud AM, Hussein OE, Hozayen WG and Abd El-Twab SM: Methotrexate hepatotoxicity is associated with oxidative stress, and down-regulation of PPAR $\gamma$  and Nrf2: Protective effect of 18 $\beta$ -Glycyrrhetic acid. *Chem Biol Interact* 270: 59-72, 2017.
- Cheng X, Qiu L and Wang F: 18 $\alpha$ -glycyrrhetic acid (GA) ameliorates fructose-induced nephropathy in mice by suppressing oxidative stress, dyslipidemia and inflammation. *Biomed Pharmacother* 125: 109702, 2020.
- Zhou J, Cai W, Jin M, Xu J, Wang Y, Xiao Y, Hao L, Wang B, Zhang Y, Han J and Huang R: 18 $\beta$ -glycyrrhetic acid suppresses experimental autoimmune encephalomyelitis through inhibition of microglia activation and promotion of remyelination. *Sci Rep* 5: 13713, 2015.
- Oztanir MN, Ciftci O, Cetin A, Durak MA, Basak N and Akyuva Y: The beneficial effects of 18 $\beta$ -glycyrrhetic acid following oxidative and neuronal damage in brain tissue caused by global cerebral ischemia/reperfusion in a C57BL/6 mouse model. *Neurol Sci* 35: 1221-1228, 2014.
- Kao TC, Shyu MH and Yen GC: Glycyrrhizic acid and 18 $\beta$ -glycyrrhetic acid inhibit inflammation via PI3K/Akt/GSK3 $\beta$  signaling and glucocorticoid receptor activation. *J Agric Food Chem* 58: 8623-8629, 2010.
- Gao L, Feng A, Yue P, Liu Y, Zhou Q, Zang Q and Teng J: LncRNA BC083743 promotes the proliferation of Schwann cells and axon regeneration through miR-103-3p/BDNF after sciatic nerve crush. *J Neuropathol Exp Neurol* 79: 1100-1114, 2020.
- Chi GF, Kim DW, Jiang MH, Yoon KJ and Son Y: Schwann-like cells from human melanocytes and their fate in sciatic nerve injury. *Neuroreport* 22: 603-608, 2011.
- Wang L, Sanford MT, Xin Z, Lin G and Lue TF: Role of Schwann cells in the regeneration of penile and peripheral nerves. *Asian J Androl* 17: 776-782, 2015.
- Gonçalves NP, Mohseni S, El Soury M, Ulrichsen M, Richner M, Xiao J, Wood RJ, Andersen OM, Coulson EJ, Raimondo S, et al: Peripheral nerve regeneration is independent from schwann cell p75<sup>NTR</sup> expression. *Front Cell Neurosci* 13: 235, 2019.
- Gomez-Sanchez JA, Pilch KS, van der Lans M, Fazal SV, Benito C, Wagstaff LJ, Mirsky R and Jessen KR: After nerve injury, lineage tracing shows that myelin and remak schwann cells elongate extensively and branch to form repair Schwann cells, which shorten radically on remyelination. *J Neurosci* 37: 9086-9099, 2017.
- Julien O and Wells JA: Caspases and their substrates. *Cell Death Differ* 24: 1380-1389, 2017.
- Kalkavan H and Green DR: MOMP, cell suicide as a BCL-2 family business. *Cell Death Differ* 25: 46-55, 2018.
- Li ZY, Tung YT, Chen SY and Yen GC: Novel findings of 18 $\beta$ -glycyrrhetic acid on sRAGE secretion through inhibition of transient receptor potential canonical channels in high-glucose environment. *Biofactors* 45: 607-615, 2019.
- Wankun X, Wenzhen Y, Min Z, Weiyan Z, Huan C, Wei D, Lvzhen H, Xu Y and Xiaoxin L: Protective effect of paeoniflorin against oxidative stress in human retinal pigment epithelium in vitro. *Mol Vis* 17: 3512-3522, 2011.
- Livak KJ and Schmittgen TD: Analysis of relative gene expression data using real-time quantitative PCR and the 2(-Delta Delta C(T)) method. *Methods* 25: 402-408, 2001.
- Zhang D, Sun J, Yang B, Ma S, Zhang C and Zhao G: Therapeutic effect of tetrapanax papyriferus and hederagenin on chronic neuropathic pain of chronic constriction injury of sciatic nerve rats based on KEGG pathway prediction and experimental verification. *Evid Based Complement Alternat Med* 2020: 2545806, 2020.
- Gouin O, L'Hérondelle K, Lebonvallet N, Le Gall-Ianotto C, Sakka M, Buhé V, Plée-Gautier E, Carré JL, Lefeuvre L, Misery L and Le Garrec R: TRPV1 and TRPA1 in cutaneous neurogenic and chronic inflammation: Pro-inflammatory response induced by their activation and their sensitization. *Protein Cell* 8: 644-661, 2017.
- Wang M, Zhang Y, Xu M, Zhang H, Chen Y, Chung KF, Adcock IM and Li F: Roles of TRPA1 and TRPV1 in cigarette smoke-induced airway epithelial cell injury model. *Free Radic Biol Med* 134: 229-238, 2019.
- Ma G, Luo W, Lu J, Ma DL, Leung CH, Wang Y and Chen X: Cucurbitacin E induces caspase-dependent apoptosis and protective autophagy mediated by ROS in lung cancer cells. *Chem Biol Interact* 253: 1-9, 2016.
- Kang N, Wang MM, Wang YH, Zhang ZN, Cao HR, Lv YH, Yang Y, Fan PH, Qiu F and Gao XM: Tetrahydrocurcumin induces G2/M cell cycle arrest and apoptosis involving p38 MAPK activation in human breast cancer cells. *Food Chem Toxicol* 67: 193-200, 2014.
- Sun Y, Liu WZ, Liu T, Feng X, Yang N and Zhou HF: Signaling pathway of MAPK/ERK in cell proliferation, differentiation, migration, senescence and apoptosis. *J Recept Signal Transduct Res* 35: 600-604, 2015.
- Coskun AK, Yigiter M, Oral A, Odabasoglu F, Halici Z, Menten O, Cadirci E, Atalay F and Suleyman H: The effects of montelukast on antioxidant enzymes and proinflammatory cytokines on the heart, liver, lungs, and kidneys in a rat model of cecal ligation and puncture-induced sepsis. *ScientificWorldJournal* 11: 1341-1356, 2011.
- Ishida T, Mizushima Y, Yagi S, Irino Y, Nishiumi S, Miki I, Kondo Y, Mizuno S, Yoshida H, Azuma T and Yoshida M: Inhibitory effects of glycyrrhetic acid on DNA polymerase and inflammatory activities. *Evid Based Complement Alternat Med* 2012: 650514, 2012.
- Ishida T, Miki I, Tanahashi T, Yagi S, Kondo Y, Inoue J, Kawachi S, Nishiumi S, Yoshida M, Maeda H, et al: Effect of 18 $\beta$ -glycyrrhetic acid and hydroxypropyl  $\gamma$ -cyclodextrin complex on indomethacin-induced small intestinal injury in mice. *Eur J Pharmacol* 714: 125-131, 2013.
- Khezri MK, Turkkan A, Koc C, Salman B, Levent P, Cakir A, Kafa IM, Cansev M and Bekar A: Anti-apoptotic and anti-oxidant effects of systemic uridine treatment in an experimental model of sciatic nerve injury. *Turk Neurosurg* 31: 373-378, 2021.
- Zhang D, Yang B, Chang SQ, Ma SS, Sun JX, Yi L, Li X, Shi HM, Jing B, Zheng YC, et al: Protective effect of paeoniflorin on H<sub>2</sub>O<sub>2</sub> induced Schwann cells injury based on network pharmacology and experimental validation. *Chin J Nat Med* 19: 90-99, 2021.
- Kalinski AL, Yoon C, Huffman LD, Duncker PC, Kohen R, Passino R, Hafner H, Johnson C, Kawaguchi R, Carbajal KS, et al: Analysis of the immune response to sciatic nerve injury identifies efferocytosis as a key mechanism of nerve debridement. *Elife* 9: e60223, 2020.



This work is licensed under a Creative Commons Attribution-NonCommercial-NoDerivatives 4.0 International (CC BY-NC-ND 4.0) License.